

Controlling Condensate Collapse and Expansion with an Optical Feshbach Resonance

Mi Yan, B. J. DeSalvo, B. Ramachandhran, H. Pu, and T. C. Killian

Department of Physics and Astronomy, Rice University, Houston, Texas 77251, USA

(Received 7 September 2012; published 20 March 2013)

We demonstrate control of the collapse and expansion of an ^{88}Sr Bose-Einstein condensate using an optical Feshbach resonance near the $^1S_0\text{-}^3P_1$ intercombination transition at 689 nm. Significant changes in dynamics are caused by modifications of scattering length by up to $\pm 10a_{\text{bg}}$, where the background scattering length of ^{88}Sr is $a_{\text{bg}} = -2a_0$ ($a_0 = 0.053$ nm). Changes in scattering length are monitored through changes in the size of the condensate after a time-of-flight measurement. Because the background scattering length is close to zero, blue detuning of the optical Feshbach resonance laser with respect to a photoassociative resonance leads to increased interaction energy and a faster condensate expansion, whereas red detuning triggers a collapse of the condensate. The results are modeled with the time-dependent nonlinear Gross-Pitaevskii equation.

DOI: [10.1103/PhysRevLett.110.123201](https://doi.org/10.1103/PhysRevLett.110.123201)

PACS numbers: 34.50.Rk, 34.50.Cx, 67.85.Hj

The ability to tune interactions in ultracold atomic gases makes these systems ideal for exploring many-body physics [1] and has enabled some of the most important recent advances in atomic physics, such as investigation of the Bose-Einstein condensate (BEC)-Bardeen-Cooper-Schrieffer crossover regime [1] and creation of quantum degenerate molecules [2,3]. Magnetic Feshbach resonances [4], which are the standard tool for changing atomic interactions, have proven incredibly powerful, but they are also limited because the methods for creating magnetic fields preclude high-frequency spatial and temporal modulation. Also, in atoms with nondegenerate ground states, such as alkaline-earth-metal atoms, magnetic Feshbach resonances do not exist.

These limitations can be overcome by using an optical Feshbach resonance (OFR), which tunes interatomic interactions by coupling a colliding atom pair to a bound molecular level of an excited state potential with a laser tuned near a photoassociative resonance [5]. Optical Feshbach resonances may open new avenues of research in nonlinear matter waves [6–8] and quantum fluids [9–11] and could be very valuable for experiments with fermionic alkaline-earth atoms [12,13] in lattices [14], which possess $SU(N)$ symmetry with large N and have attracted great attention lately because of novel thermodynamics [15–17] and predictions of frustrated magnetism and topological ground states [18–21]. Here, we present the control of collapse and expansion of an ^{88}Sr BEC with an OFR near the $^1S_0\text{-}^3P_1$ intercombination transition at 689 nm.

Early experiments on OFRs [22–24] used strong dipole-allowed transitions in alkali-metal atoms to alter atomic collision properties, but substantial change in the atom-atom scattering length was accompanied by rapid atom losses. Tuning of interactions in alkali-metal atoms, but with smaller atom loss, was recently obtained with a magnetic Feshbach resonance using an ac Stark shift of the closed channel to modify the position of the resonance

[25,26]. Recently, a multiple-laser optical method was proposed for wider modulation of the interaction strength near a magnetic Feshbach resonance [27]. Unfortunately, none of these hybrid variations are feasible for atoms lacking magnetic Feshbach resonances.

Ciurylo *et al.* [28,29] predicted that an OFR induced by a laser tuned near a weakly allowed transition should tune the scattering length with significantly less induced losses. This can be done with divalent atoms, such as strontium and ytterbium, by exciting near an intercombination transition from the singlet ground state to a metastable triplet level. The improved OFR properties result from the long lifetime of the excited molecular state and relatively large overlap integral between excited molecular and ground collisional wave functions. Intercombination-transition OFRs have been used to modify the photoassociation (PA) spectrum in a thermal gas of Yb [30], modulate the mean field energy in a Yb BEC in an OFR-laser standing wave [31], and modify thermalization and loss rates in a thermal gas of ^{88}Sr [32]. In the OFR work with an Yb BEC [31], small detunings from a molecular resonance were used ($|\Delta| < 10\Gamma_{\text{mol}}$, where Γ_{mol} is the natural decay rate of the excited molecular level), which led to short sample lifetimes on the order of microseconds. Longer exposure times and detunings $|\Delta| < 50\Gamma_{\text{mol}}$ were used in thermal Sr gases [32], but at much lower atomic density than typically found in a degenerate sample.

There is great interest in intercombination-line OFRs at much larger detuning in quantum degenerate gases of divalent atoms [12,33–35], with the goal of modifying the scattering length and still maintaining sample lifetimes on the order of dynamical time scales of quantum fluids [10,11]. Here we use an OFR to control collapse and expansion of an ^{88}Sr condensate during time-of-flight measurements. ^{88}Sr has an s -wave background scattering length of $a_{\text{bg}} = -2a_0$ [36,37], which allows convenient modification of the scattering length to either positive or

more negative values. A large relative change in scattering length $a_{\text{opt}}/a_{\text{bg}} = \pm 10$ is demonstrated, with the loss rate constant $K_{\text{in}} \sim 10^{-12} \text{ cm}^3/\text{s}$ comparable to that of Ref. [26]. We explore $|\Delta|$ values as large as $667\Gamma_{\text{mol}}$ and obtain sample lifetimes of milliseconds during the application of the OFR beam.

According to the isolated resonance model [28,29], a laser of wavelength λ detuned by Δ from a photoassociative transition to an excited molecular state $|n\rangle$ modifies the atomic scattering length according to $a = a_{\text{bg}} + a_{\text{opt}}$ and induces two-body inelastic collisional losses described by the loss rate constant K_{in} , where

$$a_{\text{opt}} = \frac{\ell_{\text{opt}}\Gamma_{\text{mol}}\Delta}{\Delta^2 + \frac{(\eta\Gamma_{\text{mol}})^2}{4}}, \quad K_{\text{in}} = \frac{2\pi\hbar}{\mu} \frac{\ell_{\text{opt}}\eta\Gamma_{\text{mol}}^2}{\Delta^2 + \frac{(\eta\Gamma_{\text{mol}} + \Gamma_{\text{stim}})^2}{4}}. \quad (1)$$

K_{in} is defined such that it contributes to the evolution of density n as $\dot{n} = -K_{\text{in}}n^2$ for a BEC. The optical length ℓ_{opt} , which characterizes the strength of the OFR, is defined as

$$\ell_{\text{opt}} = \frac{\lambda^3 \langle n|\varepsilon_r\rangle^2 I}{16\pi ck_r}, \quad (2)$$

where c is the speed of light, I is the intensity of the OFR beam, and k_r is the wave number for colliding atoms, given by $k_r = \sqrt{21/8}/(2R_{\text{TF}})$ for a BEC with Thomas-Fermi radius R_{TF} , and $k_r = \sqrt{2\mu\varepsilon_r}/\hbar$ for a thermal gas, where $\mu = m/2$ is the reduced mass for the atomic mass m , ε_r is the kinetic energy of the colliding atom pair, and \hbar is the reduced Planck constant. The Franck-Condon factor per unit energy for the free-bound PA transition is $|\langle n|\varepsilon_r\rangle|^2$. Because $|\langle n|\varepsilon_r\rangle|^2 \sim k_r$ in the ultracold regime [38], following the Wigner threshold law, ℓ_{opt} is independent of the collision energy. $\Gamma_{\text{mol}} = 2\pi \times 15 \text{ kHz}$ is the natural linewidth of the excited molecular level, and $\Gamma_{\text{stim}} = 2k_r\ell_{\text{opt}}\Gamma_{\text{mol}}$ is the laser-stimulated linewidth. The parameter $\eta > 1$ accounts for enhanced molecular losses, as observed in previous OFR experiments [23,32].

As shown through coupled channels calculations [32], the isolated-resonance-model expressions [Eq. (1)] break down at large detunings from photoassociative resonance. The induced scattering length a_{opt} crosses zero between resonances. Outside approximately 100 linewidths from photoassociative resonance, the two-body loss is expected to make a transition to a broad background value that varies as $1/\delta^2$, where δ is 2π times the detuning from atomic resonance [32]. A rigorous theoretical description for loss in this regime is lacking, but the underlying mechanism is collisions involving a ground-state atom and an atom excited in the wings of the atomic line. In the regime where molecular levels are unresolved, such as in light-assisted collisions in a magneto-optical trap, this loss is often described with the classical Gallagher-Pritchard model [39]. In a coupled channels description, the background loss rate is sensitive to a cutoff atom-atom distance inside

of which radiative loss is turned on, which is introduced as an *ad hoc* parameter [40]. Our measurements could provide some experimental input to determine this cutoff distance. We find the isolated-resonance-model expressions [Eq. (1)] useful for describing our measurements with the modification that the total loss rate constant is given by $K_{\text{total}} = K_{\text{in}} + K_b$, where the background loss is described phenomenologically in our regime as $K_b = K_0[\Gamma_{\text{mol}}/(2\delta)]^2$.

To probe the change in scattering length and loss, we monitor expansion of an ^{88}Sr BEC after release from the optical dipole trap (ODT) with time-of-flight absorption imaging using the $^1S_0 \rightarrow ^1P_1$ transition. Details of the formation of an ^{88}Sr BEC are given in Ref. [35]. We create condensates with about 7000 atoms, size $\sigma_0 = 0.8 \mu\text{m}$, and peak density $n_0 = 1 \times 10^{15} \text{ cm}^{-3}$. About 10% of the trapped atoms are in the condensate, and this represents about 95% of the critical number for collapse with the background scattering length of ^{88}Sr for our ODT, which is close to spherically symmetric with the geometric mean of the trap oscillation frequency $\bar{\omega} = 2\pi \times (60 \pm 5) \text{ Hz}$ [41]. The 689 nm OFR laser beam is tuned near the photoassociative transition to the second least bound vibrational level on the $^1S_0 + ^3P_1$ molecular potential, which has the binding energy of $h \times 24 \text{ MHz}$ [42].

The OFR laser, with a beam waist of $725 \mu\text{m}$, is applied to the condensate $20 \mu\text{s}$ before extinguishing the ODT and left on for a variable time τ during expansion. The exposure time in the ODT is short enough that the initial density distribution of the condensate reflects the ODT potential and the background scattering length, whereas the expansion dynamics is sensitive to the interaction energy determined by $a = a_{\text{bg}} + a_{\text{opt}}$.

Figure 1 shows one-dimensional slices through absorption images of atoms after a 35 ms time of flight with and without application of the OFR laser. Absorption images measure the areal density, which is fit with a bimodal function including a Bose distribution for the thermal atoms and a narrow Gaussian density distribution for the

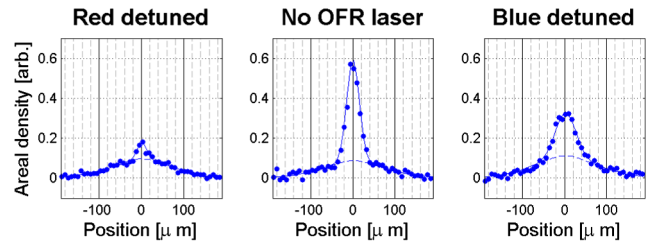


FIG. 1 (color online). Line profiles through absorption images showing OFR-induced variation of BEC expansion. Data correspond to no OFR laser and an OFR laser blue and red detuned by 0.5 MHz with respect to the -24 MHz PA line [42] applied for $\tau = 1.2 \text{ ms}$. Expansion times are 35 ms. Fits are a Bose distribution for the thermal atoms (dashed line) and a Gaussian density distribution for the BEC.

BEC, $n(r) = N_0/(2\pi\sigma^2) \exp\{-[r^2/(2\sigma^2)]\}$, to determine the number of atoms in the BEC N_0 and BEC size σ . (Quoted sizes reflect correction for imaging system resolution, which is modeled by a point spread function $L(r) = 1/(2\pi s^2) \exp\{-[r^2/(2s^2)]\}$ with $s = 5 \pm 1 \mu\text{m}$.) The condensate size after a long time of flight is a good probe of interactions because of the sensitivity to the initial interaction energy.

To obtain a qualitative understanding of the data, one can calculate the total energy immediately after the trap is extinguished using the condensate energy functional [43,44] assuming a Gaussian density for the BEC in the ODT with initial size σ_0 . When atom losses are negligible, this energy can be equated to the total kinetic energy when the condensate has expanded to a low density to give

$$N_0 \frac{3}{2} m \sigma_v^2 = N_0 \frac{3}{8} \frac{\hbar^2}{m \sigma_0^2} + N_0^2 \frac{g}{2(4\pi)^{3/2} \sigma_0^3}. \quad (3)$$

The first and second terms on the right-hand side are the kinetic energy and interaction energy in the trap before release, respectively, for $g = 4\pi\hbar^2 a/m$. The rms velocity is given by σ_v , which can be related to the BEC size after a long expansion time t through $\sigma = \sigma_v t$. A blue OFR laser detuning near the -24 MHz PA line [42] increases a , leading to more interaction energy and larger expansion velocity and BEC size. Red detuning produces the opposite behavior. When the total energy becomes negative, this simple explanation breaks down, and one observes condensate collapse and significant loss of condensate atoms.

In Fig. 2, we study the variation of the BEC size and number with the exposure time τ for several blue detunings of the OFR laser. We observe that several ms is required for full conversion of the interaction energy into kinetic energy, with larger detuning and smaller optically induced scattering length requiring longer τ times. We can estimate the time scale for conversion with a hydrodynamic description of the condensate dynamics [44]. The acceleration of atoms during expansion arises from the interaction pressure $P = gn(r)^2/2$, and a characteristic acceleration \tilde{a} can be approximated from $mn(r)\tilde{a} \approx -\nabla P \approx -n(r)\nabla[gn(r)]$. This yields $\tilde{a} = -\nabla[gn(r)]/m \sim gn_0/m\sigma_0$. In the large $N_0 a/a_{\text{ho}}$ limit with $a_{\text{ho}} = [\hbar/(m\bar{v})]^{1/2}$, one can neglect the kinetic-energy term in Eq. (3) to find the characteristic final velocity given by the conservation of energy, $v_f \sim \sigma_v \sim \sqrt{gn_0/m}$. This implies a conversion time scale $v_f/\tilde{a} \sim \sigma_0 \sqrt{m/(gn_0)}$ of 1 ms for a_{opt} of $10a_0$, which roughly matches observations. Losses from single-atom light scattering preclude leaving the OFR beam on during the entire expansion time, and knowledge of the time required for close to full conversion is helpful for interpreting the results of experiments in which we apply the OFR laser for a fixed interaction time and vary the detuning, which will be discussed below.

To quantitatively analyze the variation of size and atom number versus interaction time and extract OFR

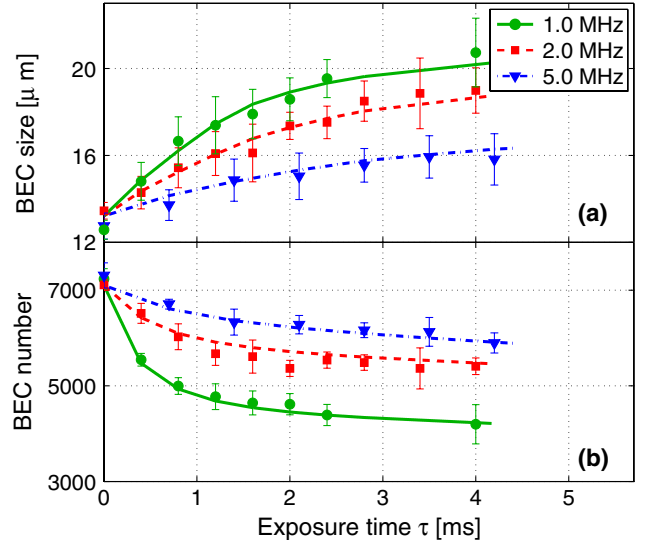


FIG. 2 (color online). (a) BEC size after 35 ms of expansion versus the exposure time of the OFR laser with the intensity of 0.057 W/cm^2 and three different detunings from the -24 MHz PA line. (b) Number of condensate atoms versus exposure time. Curves calculated by the Gross-Pitaevskii equation correspond to a combined fit of the data, yielding $\eta = 19.5$, $\ell_{\text{opt}}/I = 2.2 \times 10^4 a_0/(\text{W/cm}^2)$, and $K_0 = 5.8 \times 10^{-7} \text{ cm}^3/\text{s}$. Error bars represent the standard deviation of the mean from multiple measurements.

parameters, it is necessary to treat dynamics and atom loss with the time-dependent nonlinear Gross-Pitaevskii equation, including the effects of a_{opt} , K_{total} , and single-atom light scattering and neglecting effects of thermal atoms. The fit parameters are ℓ_{opt}/I , η , and K_0 . The rate of atomic light scattering varies from 12 to 17 s^{-1} and is included in the simulation assuming every scattering event results in the loss of one atom.

The fits are shown in Fig. 2. The data at largest detuning from photoassociative resonance strongly determine the background loss because loss from the OFR is small there. The fit optical length is $\ell_{\text{opt}}/I = (2.2 \pm 1.0) \times 10^4 a_0/(\text{W/cm}^2)$, and the fit parameter $K_0 = (5.8 \pm 1.3) \times 10^{-7} \text{ cm}^3/\text{s}$. Loss from the OFR is described by ℓ_{opt} and $\eta = 19.5^{+8}_{-3}$, and there is strong anticorrelation between ℓ_{opt} and η . The uncertainty is dominated by systematic uncertainty in the trap oscillation frequency and imaging resolution. These results are in good agreement with the measured value $\ell_{\text{opt}}/I = 1.58 \times 10^4 a_0/(\text{W/cm}^2)$ and disagree slightly with $\ell_{\text{opt}}/I = 8.3 \times 10^3 a_0/(\text{W/cm}^2)$ calculated directly from knowledge of the molecular potentials [32].

Experiments with a thermal strontium gas [32] found larger losses associated with an OFR than described by theory, which was described by $\eta = 2.7$. These measurements probed the core of the photoassociative transition ($|\Delta| < 50\Gamma_{\text{mol}}$). The additional loss is not well understood. We see a similar resonance width in a BEC when we

significantly reduce the laser intensity and interaction time and take a photoassociative loss spectrum of this core region. Our use of the OFR probes the distant wings ($50\Gamma_{\text{mol}} < \Delta < 667\Gamma_{\text{mol}}$), and a fit of the loss using the single resonance model requires an even larger value of η . We interpret the varying η values as meaning that the full spectrum of photoassociative loss, including the far wings, is not well described by a Lorentzian.

The dependence of the BEC size and number on detuning from the -24 MHz PA line is shown in Fig. 3 for a fixed intensity and interaction time $\tau = 4$ ms. The fit parameters from Fig. 2 describe the data well over this range. Note that the number of atoms initially increases with blue detuning from PA resonance as the loss from the OFR (K_{in}) decreases. The number then slowly decreases because the background loss (K_b) increases, approaching atomic resonance. The BEC size data predicted by Eq. (3), which neglects atom loss and assumes that the OFR laser is applied long enough to fully convert interaction energy into kinetic energy, is also shown in Fig. 3(a). The difference between this curve and the data highlights that atom loss is significant during the conversion process at smaller detunings, and the Gross-Pitaevskii equation simulation is required to describe the data. A typical total scattering length [Fig. 3(a) inset] is $a = 20a_0$ for $\Delta = 2\pi \times 1$ MHz $\approx 67\Gamma_{\text{mol}}$.

For red detuning, the OFR laser makes the scattering length more negative and triggers a collapse of the condensate, which is evident as a large loss in the plot of condensate number remaining after expansion [Fig. 3(b)]. The dramatic asymmetry of loss with respect to detuning

from resonance shows that the loss must reflect condensate dynamics [45–47], not photoassociative loss directly caused by the OFR laser. The Gross-Pitaevskii equation provides a good description of the BEC number data for red detuning despite the fact that the collapse dynamics may contain beyond-mean-field effects [48] not taken into account in the Gross-Pitaevskii formalism.

A variational calculation of the condensate energy functional as a function of condensate size [43,44] for the parameters of Fig. 3 predicts that the condensate expands initially after the trap is extinguished if $a > -3.8 \pm 0.2a_0$. For more negative a (-10 ± 3 MHz $< \Delta/2\pi < 0$ MHz), there is no repulsive energy barrier on the effective potential for the system and collapse results. Numerical simulation of the Gross-Pitaevskii equation supports this interpretation. Simulations show that collapse can be very nonuniform, as predicted in Ref. [45], with significant density increase only near the condensate center for a only moderately more negative than the threshold.

In summary, we have demonstrated control of collapse and expansion of an ^{88}Sr BEC using an intercombination-transition OFR. At large detuning from PA resonance ($\approx 667\Gamma_{\text{mol}}$), we obtain sample lifetimes on the order of 1 ms while changing the scattering length by 10's of a_0 . While this is a moderate change compared to the mean scattering length [49] for Sr, $\bar{a} = [4\pi/\Gamma(1/4)^2](1/2) \times (2\mu C_6/\hbar^2)^{1/4} = 75.06a_0$, it is an extremely large relative change for ^{88}Sr ($a_{\text{opt}}/a_{\text{bg}} = \pm 10$) because of the small a_{bg} . The OFR can thus drastically change the dynamics. Here, $\Gamma(x)$ is the gamma function, and $C_6 = 3170$ a.u. is the van der Waals coefficient for the interaction between two ground-state Sr atoms [50] in atomic units.

Our work probes collisions of atoms in a light field in a previously unexplored region of large detuning from photoassociative resonance. The isolated resonance model [28,29] provides a good description of the optically induced scattering length [Eq. (1)] out to a detuning of $|\Delta| \approx 667\Gamma_{\text{mol}}$ for this photoassociative transition. This is not surprising because the detuning from the PA resonance is still much less than the spacing between excited molecular states. A coupled channels numerical calculation [32] shows the breakdown of the isolated resonance approximation and absence of a significant OFR effect at comparable detuning from two PA lines. The isolated resonance model is valid over a much smaller range for describing the loss induced by the OFR laser because of the background loss and the enhanced loss parametrized by a large value of η in the far wings of the line.

The original peak density of the condensate is extremely high in our experiment because of the attractive interactions. Increased lifetime or larger OFR effect should be obtainable for densities commensurate with single-site loading of an optical lattice. Improvements could also be made by working at larger detuning from PA resonance and larger laser intensities. Working with a more deeply bound

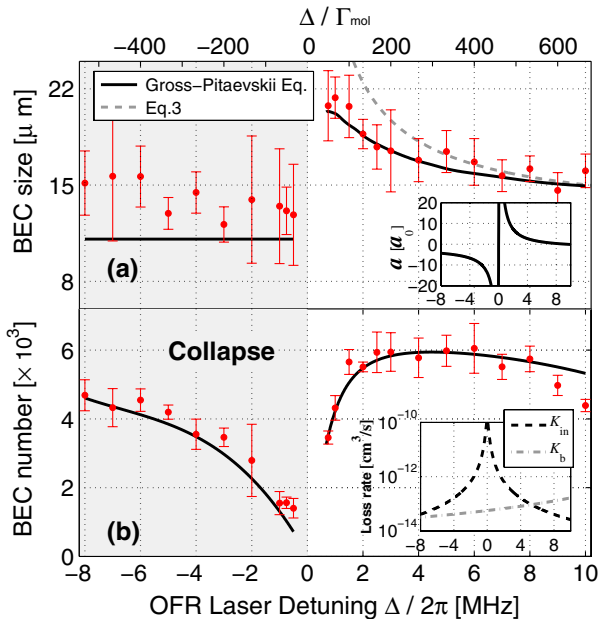


FIG. 3 (color online). The BEC size (a) and number (b) versus the detuning with respect to the -24 MHz PA resonance for an intensity of 0.057 W/cm 2 . The OFR beam is applied for 4.0 ms, and the data are recorded after 35 ms of expansion. The insets give the total scattering length a and the loss rate constants.

excited molecular state such as the PA line at -1.08 GHz [42] may offer advantages in this direction, such as greater suppression of atomic light scattering and reduced background two-body loss. This holds promise to bring many possible experiments involving optical Feshbach resonances and quantum fluids into reach.

We thank Paul Julienne for helpful discussions and acknowledge support from the Welch Foundation (C-1579 and C-1669) and the National Science Foundation (PHY-1205946 and PHY-1205973).

-
- [1] I. Bloch, J. Dalibard, and W. Zwerger, *Rev. Mod. Phys.* **80**, 885 (2008).
- [2] M. Greiner, C. A. Regal, and D. S. Jin, *Nature (London)* **426**, 537 (2003).
- [3] S. Jochim, M. Bartenstein, A. Altmeyer, G. Hendl, S. Riedl, C. Chin, J. H. Denschlag, and R. Grimm, *Science* **302**, 2101 (2003).
- [4] C. Chin, R. Grimm, P. Julienne, and E. Tiesinga, *Rev. Mod. Phys.* **82**, 1225 (2010).
- [5] P. O. Fedichev, Y. Kagan, G. V. Shlyapnikov, and J. T. M. Walraven, *Phys. Rev. Lett.* **77**, 2913 (1996).
- [6] H. Saito and M. Ueda, *Phys. Rev. Lett.* **90**, 040403 (2003).
- [7] M. I. Rodas-Verde, H. Michinel, and V. M. Pérez-García, *Phys. Rev. Lett.* **95**, 153903 (2005).
- [8] Y. V. Kartashov, B. A. Malomed, and L. Torner, *Rev. Mod. Phys.* **83**, 247 (2011).
- [9] M. P. A. Fisher, P. B. Weichman, G. Grinstein, and D. S. Fisher, *Phys. Rev. B* **40**, 546 (1989).
- [10] R. Qi and H. Zhai, *Phys. Rev. Lett.* **106**, 163201 (2011).
- [11] C.-C. Chien, *Phys. Lett. A* **376**, 729 (2012).
- [12] B. J. DeSalvo, M. Yan, P. G. Mickelson, Y. N. Martinez de Escobar, and T. C. Killian, *Phys. Rev. Lett.* **105**, 030402 (2010).
- [13] M. K. Tey, S. Stellmer, R. Grimm, and F. Schreck, *Phys. Rev. A* **82**, 011608 (2010).
- [14] S. Sugawa, K. Inaba, S. Taie, R. Yamazaki, M. Yamashita, and Y. Takahashi, *Nat. Phys.* **7**, 642 (2011).
- [15] K. R. A. Hazzard, V. Gurarie, M. Hermele, and A. M. Rey, *Phys. Rev. A* **85**, 041604 (2012).
- [16] Z. Cai, H.-h. Hung, L. Wang, D. Zheng, and C. Wu, *arXiv:1202.6323*.
- [17] S. Taie, R. Yamazaki, S. Sugawa, and Y. Takahashi, *Nat. Phys.* **8**, 825 (2012).
- [18] C. Wu, J.-P. Hu, and S.-C. Zhang, *Phys. Rev. Lett.* **91**, 186402 (2003).
- [19] M. A. Cazalilla, A. F. Ho, and M. Ueda, *New J. Phys.* **11**, 103033 (2009).
- [20] C. Honerkamp and W. Hofstetter, *Phys. Rev. Lett.* **92**, 170403 (2004).
- [21] M. Hermele, V. Gurarie, and A. M. Rey, *Phys. Rev. Lett.* **103**, 135301 (2009).
- [22] F. K. Fatemi, K. M. Jones, and P. D. Lett, *Phys. Rev. Lett.* **85**, 4462 (2000).
- [23] M. Theis, G. Thalhammer, K. Winkler, M. Hellwig, G. Ruff, R. Grimm, and J. H. Denschlag, *Phys. Rev. Lett.* **93**, 123001 (2004).
- [24] G. Thalhammer, M. Theis, K. Winkler, R. Grimm, and J. H. Denschlag, *Phys. Rev. A* **71**, 033403 (2005).
- [25] D. Bauer, M. Lettner, C. Vo, G. Rempe, and S. Durr, *Nat. Phys.* **5**, 339 (2009).
- [26] D. M. Bauer, M. Lettner, C. Vo, G. Rempe, and S. Durr, *Phys. Rev. A* **79**, 062713 (2009).
- [27] H. Wu and J. E. Thomas, *Phys. Rev. Lett.* **108**, 010401 (2012).
- [28] R. Ciurylo, E. Tiesinga, and P. S. Julienne, *Phys. Rev. A* **71**, 030701(R) (2005).
- [29] R. Ciurylo, E. Tiesinga, and P. S. Julienne, *Phys. Rev. A* **74**, 022710 (2006).
- [30] K. Enomoto, K. Kasa, M. Kitagawa, and Y. Takahashi, *Phys. Rev. Lett.* **101**, 203201 (2008).
- [31] R. Yamazaki, S. Taie, S. Sugawa, and Y. Takahashi, *Phys. Rev. Lett.* **105**, 050405 (2010).
- [32] S. Blatt, T. L. Nicholson, B. J. Bloom, J. R. Williams, J. W. Thomsen, P. S. Julienne, and J. Ye, *Phys. Rev. Lett.* **107**, 073202 (2011).
- [33] Y. N. Martinez de Escobar, P. G. Mickelson, M. Yan, B. J. DeSalvo, S. B. Nagel, and T. C. Killian, *Phys. Rev. Lett.* **103**, 200402 (2009).
- [34] S. Stellmer, M. K. Tey, B. Huang, R. Grimm, and F. Schreck, *Phys. Rev. Lett.* **103**, 200401 (2009).
- [35] P. G. Mickelson, Y. N. Martinez de Escobar, M. Yan, B. J. DeSalvo, and T. C. Killian, *Phys. Rev. A* **81**, 051601(R) (2010).
- [36] Y. N. Martinez de Escobar, P. G. Mickelson, P. Pellegrini, S. B. Nagel, A. Traverso, M. Yan, R. Côté, and T. C. Killian, *Phys. Rev. A* **78**, 062708 (2008).
- [37] A. Stein, H. Knöckel, and E. Tiemann, *Eur. Phys. J. D* **57**, 171 (2010).
- [38] J. L. Bohn and P. S. Julienne, *Phys. Rev. A* **60**, 414 (1999).
- [39] J. Weiner, *Cold and Ultracold Collisions in Quantum Microscopic and Mesoscopic Systems* (Cambridge University Press, Cambridge, England, 2003).
- [40] P. S. Julienne (private communication).
- [41] M. Yan, R. Chakraborty, A. Mazurenko, P. G. Mickelson, Y. N. Martinez de Escobar, B. J. DeSalvo, and T. C. Killian, *Phys. Rev. A* **83**, 032705 (2011).
- [42] T. Zelevinsky, M. M. Boyd, A. D. Ludlow, T. Ido, J. Ye, R. Ciurylo, P. Naidon, and P. S. Julienne, *Phys. Rev. Lett.* **96**, 203201 (2006).
- [43] V. M. Pérez-García, H. Michinel, J. I. Cirac, M. Lewenstein, and P. Zoller, *Phys. Rev. A* **56**, 1424 (1997).
- [44] F. Dalfovo, S. Giorgini, L. P. Pitaevskii, and S. Stringari, *Rev. Mod. Phys.* **71**, 463 (1999).
- [45] Y. Kagan, A. E. Muryshv, and G. V. Shlyapnikov, *Phys. Rev. Lett.* **81**, 933 (1998).
- [46] J. M. Gerton, D. Strekalov, I. Prodan, and R. G. Hulet, *Nature (London)* **408**, 692 (2000).
- [47] E. A. Donley, N. R. Claussen, S. L. Cornish, J. L. Roberts, E. A. Cornell, and C. E. Wieman, *Nature (London)* **412**, 295 (2001).
- [48] R. J. Dodd, M. Edwards, C. J. Williams, C. W. Clark, M. J. Holland, P. A. Ruprecht, and K. Burnett, *Phys. Rev. A* **54**, 661 (1996).
- [49] G. F. Gribakin and V. V. Flambaum, *Phys. Rev. A* **48**, 546 (1993).
- [50] S. G. Porsev and A. Derevianko, *Phys. Rev. A* **65**, 020701 (2002).